

Analysis in k -space of Magnetization Dynamics Driven by Strong Terahertz Fields

V. Scalera¹, M. Hudl², K. Neeraj², S. Perna¹, M. d'Aquino³, S. Bonetti², C. Serpico¹

¹Department of Electrical Engineering and ICT, University of Naples Federico II, 80125 Naples, Italy

²Department of Physics, Stockholm University, 106 91 Stockholm, Sweden

³Department of Engineering, University of Naples "Parthenope", 80143 Naples, Italy

Abstract—Demagnetization in a thin film due to a terahertz pulse of magnetic field is investigated. Linearized LLG equation in the Fourier space to describe the magnetization dynamics is derived, and spin waves time evolution is studied. Finally, the demagnetization due to spin waves dynamics and recent experimental observations on similar magnetic system are compared. As a result of it, the marginal role of spin waves dynamics in loss of magnetization is established.

Index Terms—ultrafast magnetization dynamics, demagnetization, spin waves analysis

I. INTRODUCTION

The mode of operation of magnetic storage technologies strongly relies on the control of fast magnetization reorientation in a small region of a ferromagnetic media. Thus, in order to increase the efficiency and the speed of these technologies, it is crucial to develop techniques to obtain increasingly faster magnetic dynamics. In this respect, large research efforts are currently carried out to achieve fast magnetic reorientation dynamics by using intense electromagnetic pulses [1]. In the early pioneering work in this area, femtosecond optical pulses were used to induce magnetization dynamics indirectly via electronic excitation [2], [3]. More recently, it has been shown that intense terahertz (THz) pulses can be used to achieve ultrafast magnetization dynamics by direct Zeeman coupling of magnetization with the magnetic field component of the pulse [4]. It turns out that this technique enables to approach the fastest possible magnetization reversal [6]. A surprising result of these experiments is the reduction of the magnetization module [4], even when the THz pulses have energies too small to heat the medium. Such demagnetization process has been explained in terms of ultrafast scattering of spin polarized currents [5].

In this work, the role of spin waves dynamics in the demagnetization process is investigated. In particular, the occurrence of inhomogeneities in the magnetization pattern due to spin waves excitation for a thin film excited by THz pulses, similar to the one considered in ref. [4], is evaluated. The linear regime is considered and magnetization dynamics in terms of plane waves [7], [8], [9] in the Fourier transform domain (k -space) is described. The dispersion relations are derived and the demagnetization effect due to the spin waves excitation is numerically computed and compared with experimental results. It is found that the role of spin waves induced inhomogeneities is several order of magnitude smaller than that measured in ref. [4], highlighting the importance of spin-transport phenomena in ultrafast magnetization dynamics.

II. MAGNETIZATION DYNAMICS

The system considered is a thin film where the magnetization dynamics is assumed to be described by the LLG equation, expressed by the following equation:

$$\frac{\partial \mathbf{M}}{\partial t} = \gamma \mathbf{M} \times \left(\mathbf{H}_{\text{eff}} - \frac{\alpha}{\gamma M_S} \frac{\partial \mathbf{M}}{\partial t} \right), \quad (1)$$

where γ is the gyromagnetic ratio, α is the damping constant, $\mathbf{M}(\mathbf{r}, t)$ is the magnetization, M_S is the saturation magnetization, $\mathbf{H}_{\text{eff}}(\mathbf{r}, t)$ is the effective magnetic field.

The effective magnetic field is given by the sum of several contributions according to the following equation:

$$\mathbf{H}_{\text{eff}} = \mathbf{H}_a(\mathbf{r}, t) + \mathbf{H}_M[\mathbf{M}] + \ell_{EX}^2 \nabla^2 \mathbf{M}, \quad (2)$$

where \mathbf{H}_a is the applied field, ℓ_{EX} is the exchange length, and the demagnetizing field \mathbf{H}_M is given by

$$\mathbf{H}_M(\mathbf{r}, t) = -\frac{1}{4\pi} \nabla \nabla \cdot \int_{\mathbb{R}^3} \frac{\mathbf{M}(\mathbf{s})}{|\mathbf{r} - \mathbf{s}|} d^3 \mathbf{s}. \quad (3)$$

Let the applied magnetic field be

$$\mathbf{H}_a(\mathbf{r}, t) = \mathbf{H}_{DC} + \mathbf{H}_{\text{THz}}(\mathbf{r}, t), \quad (4)$$

where \mathbf{H}_{DC} is constant in time and space, and $\mathbf{H}_{\text{THz}}(\mathbf{r}, t)$ is a pulse with sub-picosecond time duration. In the following it is considered the case where the film thickness d satisfies the relation $d \sim \ell_{EX}$. This produces that the magnetization does not change significantly along the film thickness and then makes reasonable the following assumption:

$$\mathbf{M}(\mathbf{r}, t) = \mathbf{M}(x, y, t) = \mathbf{M}(\boldsymbol{\rho}, t), \quad (5)$$

where $\boldsymbol{\rho} \in \mathbb{R}^2$ is used to denote points of the xy -plane.

In this case only the average value of magnetic field (over the film thickness) affects the magnetization dynamics, namely

$$\langle \mathbf{H}_{\text{eff}} \rangle(\boldsymbol{\rho}, t) = \frac{1}{d} \int_{-d/2}^{+d/2} \mathbf{H}_{\text{eff}}(x, y, z, t) dz. \quad (6)$$

Similarly, we define $\langle \mathbf{H}_{\text{THz}} \rangle$ and $\langle \mathbf{H}_M \rangle$ as the average over the film thickness of \mathbf{H}_{THz} and \mathbf{H}_M respectively.

At this point, it is useful to express the magnetization vector field through its Fourier transform:

$$\mathbf{M}(\boldsymbol{\rho}, t) = \frac{1}{4\pi^2} \int_{\mathbb{R}^2} \mathcal{M}(\mathbf{k}, t) \exp(i\mathbf{k} \cdot \boldsymbol{\rho}) d^2 \mathbf{k}, \quad (7)$$

which expresses the fact that the magnetization is seen as a continuous superposition of spin waves. When we apply the demagnetizing field and the exchange field operator to the

single spin wave, we obtain another spin wave with the same wave vector of the magnetization. In fact we have:

$$\langle \mathbf{H}_M \rangle [\mathcal{M}(\mathbf{k}, t) e^{i\rho \cdot \mathbf{k}}] = -D(k) \mathcal{M}(\mathbf{k}, t) e^{i\rho \cdot \mathbf{k}}, \quad (8)$$

and

$$\ell_{EX}^2 \nabla^2 (\mathcal{M}(\mathbf{k}) e^{i\rho \cdot \mathbf{k}, t}) = -k^2 \ell_{EX}^2 (\mathcal{M}(\mathbf{k}, t) e^{i\rho \cdot \mathbf{k}}), \quad (9)$$

where $k = \|\mathbf{k}\|$ and $D(k)$ is a symmetric 3×3 matrix (see appendix A).

As we will see in the following, equations (8) and (9) imply the well known fact that the linear dynamics of spin waves with different wave vectors are independent. When $\mathbf{H}_{THz}(t) = \mathbf{0}$, the equilibrium condition of (1) is satisfied by uniform magnetization and is expressed by the following Brown's equation

$$\mathbf{M}_0 \times \langle \mathbf{H}_{\text{eff},0} \rangle = \mathbf{0}. \quad (10)$$

which in scalar form reads as

$$H_{DC} \sin(\theta_H - \theta_M) - M_S \cos \theta_M \sin \theta_M = 0, \quad (11)$$

where θ_M and θ_H are the angles between the unit vector \mathbf{e}_z and the vectors \mathbf{M}_0 and \mathbf{H}_{DC} respectively.

Introducing a Cartesian coordinate system $\{\mathbf{e}_m, \mathbf{e}_\theta, \mathbf{e}_\varphi\}$, given by

$$\mathbf{e}_m = \frac{\mathbf{M}_0}{M_S}, \quad \mathbf{e}_\varphi = \frac{\mathbf{e}_z \times \mathbf{e}_m}{|\mathbf{e}_z \times \mathbf{e}_m|}, \quad \mathbf{e}_\theta = \frac{\mathbf{e}_\varphi \times \mathbf{e}_m}{|\mathbf{e}_\varphi \times \mathbf{e}_m|}, \quad (12)$$

the magnetization is written as

$$\mathbf{M}(\boldsymbol{\rho}, t) = M_S \mathbf{e}_m + M_\theta(\boldsymbol{\rho}, t) \mathbf{e}_\theta + M_\varphi(\boldsymbol{\rho}, t) \mathbf{e}_\varphi, \quad (13)$$

where $M_\theta(\boldsymbol{\rho}, t)$ and $M_\varphi(\boldsymbol{\rho}, t)$ are the first order variations. By linearizing (1) and projecting it on the plane orthogonal to \mathbf{M}_0 , it eventually yields

$$\frac{\partial M_\theta}{\partial t} - \alpha \frac{\partial M_\varphi}{\partial t} = \gamma H_0 M_\varphi - \gamma M_S H_\varphi, \quad (14)$$

$$-\alpha \frac{\partial M_\theta}{\partial t} - \frac{\partial M_\varphi}{\partial t} = \gamma H_0 M_\theta - \gamma M_S H_\theta, \quad (15)$$

where

$$H_\varphi = \langle \mathbf{H}_{\text{eff}} \rangle \cdot \mathbf{e}_\varphi, \quad H_\theta = \langle \mathbf{H}_{\text{eff}} \rangle \cdot \mathbf{e}_\theta, \quad H_0 = \|\langle \mathbf{H}_{\text{eff},0} \rangle\|.$$

In this framework the field $\langle \mathbf{H}_{THz} \rangle(\boldsymbol{\rho}, t)$ is treated as a first order perturbation.

Replacing expression (2) of the effective field (along with (9) and (8)) into (14) and (15) and taking the Fourier transform in space, we arrive to the following system of equations:

$$\frac{\partial}{\partial t} \begin{bmatrix} \mathcal{M}_\theta \\ \mathcal{M}_\varphi \end{bmatrix} = A(\mathbf{k}) \begin{bmatrix} \mathcal{M}_\theta \\ \mathcal{M}_\varphi \end{bmatrix} - \gamma M_S \begin{bmatrix} \mathcal{H}_\theta \\ \mathcal{H}_\varphi \end{bmatrix}, \quad (16)$$

where \mathcal{H}_θ and \mathcal{H}_φ are the components along \mathbf{e}_θ and \mathbf{e}_φ of the Fourier transform in space of the applied THz field, the dynamical matrix is

$$A = \begin{bmatrix} 1 & -\alpha \\ -\alpha & -1 \end{bmatrix}^{-1} \begin{bmatrix} \gamma M_S D_{\theta\varphi}(\mathbf{k}) & \gamma \hat{H}_\theta(\mathbf{k}) \\ \gamma \hat{H}_\varphi(\mathbf{k}) & \gamma M_S D_{\varphi\theta}(\mathbf{k}) \end{bmatrix}, \quad (17)$$

and

$$\hat{H}_i(\mathbf{k}) = H_0 + M_S D_{ii}(\mathbf{k}) + M_S k^2 \ell_{EX}^2. \quad (18)$$

For every \mathbf{k} , equation (16) describes a 2×2 linear system without interactions between spin waves with different \mathbf{k} . Dynamics can be simulated separately for every wave vector, whereas the magnetization in real space is obtained through (7).

At this point, it is useful to derive the dispersion relations for spin waves dynamics, which will be of help in explaining the numerical results of the next section. Dispersion relations are obtained by imposing $\det(A - i\omega I) = 0$ with $\alpha = 0$.

Two cases are considered: first, when the exchange field is negligible compared with the demagnetizing field and second, when the demagnetizing field is negligible compared to the exchange field.

Let us start with the first case. This situation occurs when the demagnetizing coefficients $D_{ij}(\mathbf{k})$ are much greater than $\ell_{EX}^2 k^2$, since $|D_{ij}| \leq 1$ and then the condition required is $\ell_{EX}^2 k^2 \ll 1$.

This type of waves are called magnetostatic waves.

Let us focus on the case with the magnetization out of plane ($\theta_M = 0$). This occurs when the applied field is out of plane and $H_a > M_S$. By replacing $H_0 = H_a - M_S$ and the demagnetizing factors with their expressions in (41), it eventually yields

$$\omega = -\gamma \sqrt{(H_a - M_S)(H_a - M_S S_k)}, \quad (19)$$

where S_k is defined in (40). The dispersion relation (19) has a positive group velocity and it is called forward magnetostatic wave [9].

Next we consider the magnetization is in plane ($\theta_M = \pi/2$), which occurs when the applied field is in plane. Replacing $H_0 = H_a$ and the expressions of the demagnetizing factors from (41) yields

$$\omega = -\gamma \sqrt{(H_a + M_S S_k)(H_a + M_S(1 - S_k) \sin^2 \phi_k)}, \quad (20)$$

where ϕ_k is the angle between \mathbf{M}_0 and \mathbf{k} . When $\phi_k = 0$, (20) has a negative group velocity and it called backward magnetostatic wave [9].

The plot of (19) and (20) are in Figure 1.

Consider now the case $\ell_{EX}^2 k^2 \gg 1$, i.e. the magnetostatic field is negligible. In this case the dispersion relation does not depend on the orientation \mathbf{k} . We have

$$\omega = -\gamma(H_0 + M_S \ell_{EX}^2 k^2). \quad (21)$$

For spatially uniform, or nearly uniform, terahertz pulse distribution ($kd \ll 1$) the resonance frequencies for spin waves excitation are in the order of ~ 10 GHz. Therefore, it is expected that the nonlinear spin waves dynamics regime is not reached, even for high power magnetic field pulse used for the experimental investigations of ref. [4].

III. SIMULATION

We consider a system similar to the one used in [4]: The specimen is a thin film with thickness $d = 5$ nm, the material parameters are $\mu_0 M_S = 1.84$ T, $\gamma = -176$ rad/(T · ns), $\alpha = -0.007$ and $\ell_{EX} = 4.4$ nm, and the applied magnetic field out of plane component $\mu_0 H_\perp = 0.448$ T whereas the in plane component is $\mu_0 H_\parallel = 0.056$ T. The terahertz field is

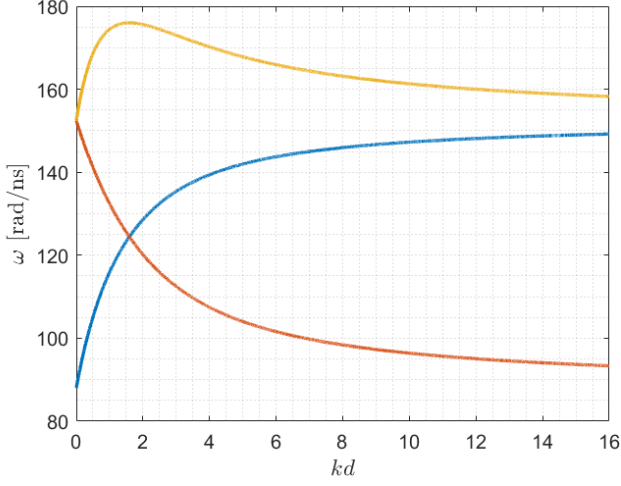


Fig. 1. Dispersion relations of magnetostatic waves ($\ell_{EX} = 0$). The saturation magnetization is $\mu_0 M_S = 1$ T and the applied field at the equilibrium is $\mu_0 H_0 = 0.5$ T, i.e. the applied field is $\mu_0 H_a = 0.5$ T for the magnetization in plane and $\mu_0 H_a = 1.5$ T for the magnetization out of plane. The blue curve is represents (19), the red and yellow curves represent (20) for $\phi_k = 0$ and $\phi_k = \pi/2$ respectively.

applied in plane (orthogonally to the constant field) and the intensity is

$$H_{THz}(\boldsymbol{\rho}, t) = \frac{H_{\text{Max}}}{\sigma_t^2} (t^2 - \sigma_t^2) \exp\left(-\frac{t^2}{2\sigma_t^2} - \frac{\rho^2}{2\sigma_x^2}\right), \quad (22)$$

where $\mu_0 H_{\text{Max}} = 0.06$ T, $\sigma_x = 500$ μm and $\sigma_t = 0.5$ ps. The time evolution of H_{THz} is displayed in the left panel of Figure 2.

The system (16) is simulated within a range of wave number

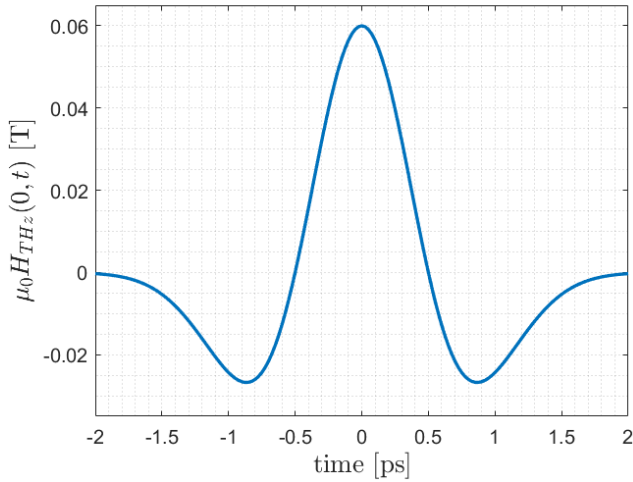


Fig. 2. Time profile of the applied terahertz pulse.

up to 10^{-5} nm^{-1} , higher wave numbers are not excited by the applied field. The time evolution of $\mathcal{M}(\mathbf{k}, t)$ is shown Figure 5 for several values of \mathbf{k} .

In the range of wave vector excited the dynamics does not change appreciably, hence the space profile of either \mathcal{M}_θ and

\mathcal{M}_φ are almost the same as $H_{THz}(\boldsymbol{\rho}, 0)$ rescaled. The space dependence of \mathcal{M}_θ and \mathcal{M}_φ are in Figure 3.

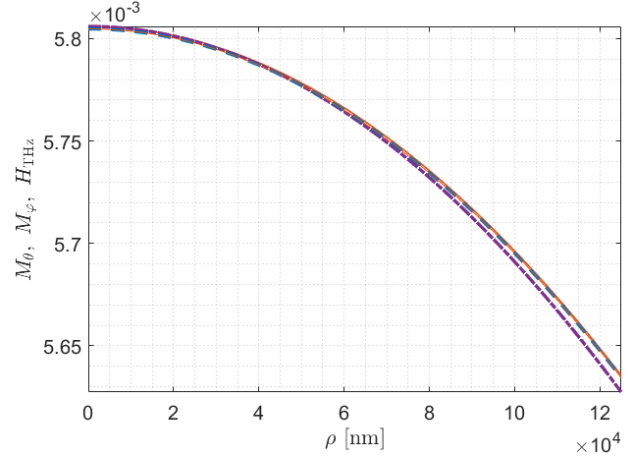


Fig. 3. Space dependence of the applied terahertz field H_{THz} and the perturbation of the magnetization M_θ and M_φ . The red solid line is M_θ , the dashed blue line is M_φ and the dashed purple line is H_{THz} . The plot are rescaled so that the in $\rho = 0$ the three curves have the same value.

In order to evaluate the demagnetization observed the magnetization is normalized, since the linearized model does not preserve the magnetization modulus. We have

$$\mathbf{M} = M_S \frac{\mathbf{M}_0 + M_\theta \mathbf{e}_\theta + M_\varphi \mathbf{e}_\varphi}{\|\mathbf{M}_0 + M_\theta \mathbf{e}_\theta + M_\varphi \mathbf{e}_\varphi\|} = M_S \frac{\mathbf{M}_0 + \delta\mathbf{M}}{\|\mathbf{M}_0 + \delta\mathbf{M}\|}, \quad (23)$$

where $\delta\mathbf{M} = M_\theta \mathbf{e}_\theta + M_\varphi \mathbf{e}_\varphi$.

The measured magnetization is given by

$$M_{\text{meas}} = \frac{1}{|\Omega_M|} \left\| \int_{\Omega_M} \mathbf{M} \, dS \right\| \quad (24)$$

where Ω_M is the area hit by the probe, i.e. a circular area with radius 125 μm , and $|\Omega_M|$ is the measure of the area.

Developing the Taylor series up to the second order in $\delta\mathbf{M}/M_S$ and using $\mathbf{M}_0 \perp \delta\mathbf{M}$, the integral is approximated by

$$\int_{\Omega_M} \mathbf{M} \, dS \approx \int_{\Omega_M} \left(\mathbf{M}_0 - \frac{\mathbf{M}_0}{2} \left\| \frac{\delta\mathbf{M}}{M_S} \right\|^2 + \delta\mathbf{M} \right) dS. \quad (25)$$

By replacing (25) in (23), neglecting the terms of order greater than two in $\delta\mathbf{M}/M_S$, we eventually obtain the demagnetization

$$M_{\text{meas}} = \sqrt{M_S^2 - I_2 + I_1}, \quad (26)$$

where

$$I_1 = \frac{1}{|\Omega_M|^2} \left(\int_{\Omega_M} \delta\mathbf{M} \, dS \right)^2, \quad (27)$$

and

$$I_2 = \frac{1}{|\Omega_M|} \int_{\Omega_M} \delta\mathbf{M}^2 \, dS. \quad (28)$$

It is noteworthy that $I_2 \geq I_1$ because of Cauchy-Schwartz inequality, hence the measured magnetization can only be smaller than M_S .

The plot of the relative reduction of the measured magnetization is displayed in Figure 4.

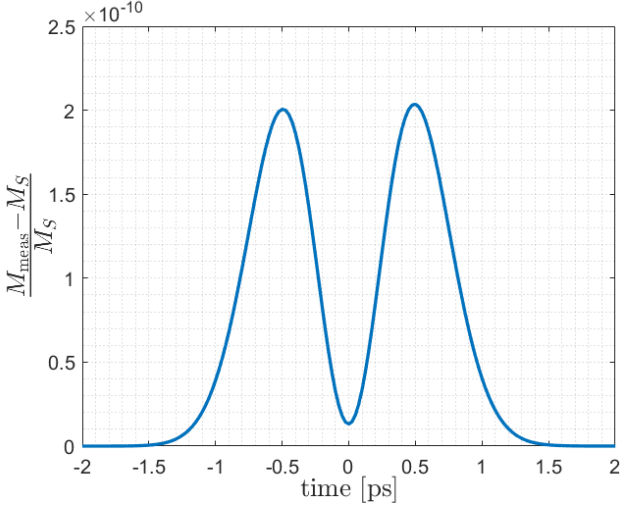


Fig. 4. Relative reduction of the measured magnetization.

Remarkably, the reduction of the observed magnetization does not grow over $2.5 \cdot 10^{-10}$, whereas the demagnetization observed in [4] is several order of magnitude higher (roughly $2 \cdot 10^{-3}$).

IV. CONCLUSION

In conclusion, the demagnetization effect induced in a thin film excited by a strong terahertz pulse is investigated. The magnetization dynamics is described in terms of linear spin waves dynamics governed by the linearized LLG projected into the Fourier's k -space. In this micromagnetic framework, we tried to reproduce the experiment described in [4] and determine whether the spin waves play a role in the experimental observed demagnetization explained in terms of ultrafast scattering of spin polarized currents [5]. It is found, that the reduction of the magnetization module computed in the simulation is several orders of magnitudes smaller than the demagnetization observed in the experiments. Moreover, despite the field intensity is high, the pulse is so short that the magnetization barely moves from equilibrium and spin waves do not grow enough to cause relevant nonlinear effects [7], [8]. Then, the magnetization reduction due to non-uniformities is negligible and the role of ultrafast spin-transport phenomenon is prevalent.

APPENDIX A

DEMAGNETIZING COEFFICIENTS COMPUTATION

This section derives the analytical expressions for the demagnetizing factor $D(\mathbf{k})$ defined in equation (8). Its elements express the linear relation between the averaged demagnetizing field and the magnetization

$$\begin{bmatrix} \langle H_{Mx} \rangle \\ \langle H_{My} \rangle \\ \langle H_{Mz} \rangle \end{bmatrix} = - \begin{bmatrix} D_{xx} & D_{xy} & D_{xz} \\ D_{xy} & D_{yy} & D_{yz} \\ D_{xz} & D_{yz} & D_{zz} \end{bmatrix} \begin{bmatrix} M_x \\ M_y \\ M_z \end{bmatrix}. \quad (29)$$

The $D_{ij}(\mathbf{k})$ can be obtained from (3), which is the general solution of the magnetostatic problem

$$\nabla \times \mathbf{H}_M = 0, \quad \nabla \cdot \mathbf{H}_M = -\nabla \cdot \mathbf{M}. \quad (30)$$

Alternatively, the system (30) can be restated in terms of a scalar potential ψ , that is

$$\mathbf{H}_M = -\nabla\psi, \quad \nabla^2\psi = \nabla \cdot \mathbf{M}. \quad (31)$$

Let us focus on the demagnetizing field in the thin film with magnetization given by

$$\mathbf{M}(\mathbf{r}) = \begin{cases} \mathbf{M}_0 \exp(i\mathbf{k} \cdot \boldsymbol{\rho}) & \text{if } |z| \leq d/2 \\ 0 & \text{if } |z| > d/2 \end{cases}. \quad (32)$$

The particular solution of (31) is

$$\psi_p(\mathbf{r}) = \begin{cases} \frac{\mathbf{k} \cdot \mathbf{M}_0}{ik^2} \exp(i\mathbf{k} \cdot \boldsymbol{\rho}) & \text{if } |z| \leq d/2 \\ 0 & \text{if } |z| > d/2 \end{cases}. \quad (33)$$

The potential (33) does not satisfy the interface conditions on the thin film surfaces, namely the continuity of the normal component of the magnetic density flux

$$(\mathbf{H}_M^m(\mathbf{r}, t) + \mathbf{M}(\mathbf{r}, t)) \cdot \mathbf{e}_z = \mathbf{H}_M^a(\mathbf{r}, t) \cdot \mathbf{e}_z, \quad (34)$$

and the continuity of the tangent component of the magnetic field

$$\mathbf{H}_M^m(\mathbf{r}, t) \times \mathbf{e}_z = \mathbf{H}_M^a(\mathbf{r}, t) \times \mathbf{e}_z, \quad (35)$$

where the superscript 'm' and 'a' denote the fields in the magnetic medium and in the air respectively, and equations (34) and (35) are imposed at $z = \pm d/2$.

The solution of (31) is obtained by summing to (33) a linear combination of harmonic functions

$$\psi_{\pm}(\mathbf{r}) = \exp(i\mathbf{k} \cdot \boldsymbol{\rho} \pm kz). \quad (36)$$

The homogeneous solution is

$$\psi_0(\mathbf{r}) = \begin{cases} C_1\psi_- & \text{if } z > d/2 \\ C_2\psi_- + C_3\psi_+ & \text{if } |z| \leq d/2 \\ C_4\psi_+ & \text{if } z < -d/2 \end{cases}, \quad (37)$$

where C_1, C_2, C_3 and C_4 are constant to be determined.

By using (34) and (35), we obtain a set of linear equations in C_1, C_2, C_3 and C_4 , which yields

$$\begin{aligned} C_1 &= -\frac{\sinh(kd/2)}{k} [(\mathbf{M}_0 \cdot \mathbf{e}_k) + (\mathbf{M}_0 \cdot \mathbf{e}_z)], \\ C_2 &= \frac{\exp(-kd/2)}{2k} [(\mathbf{M}_0 \cdot \mathbf{e}_k) + (\mathbf{M}_0 \cdot \mathbf{e}_z)], \\ C_3 &= \frac{\exp(-kd/2)}{2k} [(\mathbf{M}_0 \cdot \mathbf{e}_k) - (\mathbf{M}_0 \cdot \mathbf{e}_z)], \\ C_4 &= -\frac{\sinh(kd/2)}{k} [(\mathbf{M}_0 \cdot \mathbf{e}_k) - (\mathbf{M}_0 \cdot \mathbf{e}_z)], \end{aligned} \quad (38)$$

where $\mathbf{e}_k = (1/k)\mathbf{k}$.

The derivation of the averaged demagnetizing field is straightforward. We eventually have

$$\langle \mathbf{H}_M \rangle = -[(\mathbf{M}_0 \cdot \mathbf{e}_z)S_k + (\mathbf{M}_0 \cdot \mathbf{e}_k)(1 - S_k)] \exp(i\mathbf{k} \cdot \boldsymbol{\rho}), \quad (39)$$

where

$$S_k = [1 - \exp(-kd)]/kd. \quad (40)$$

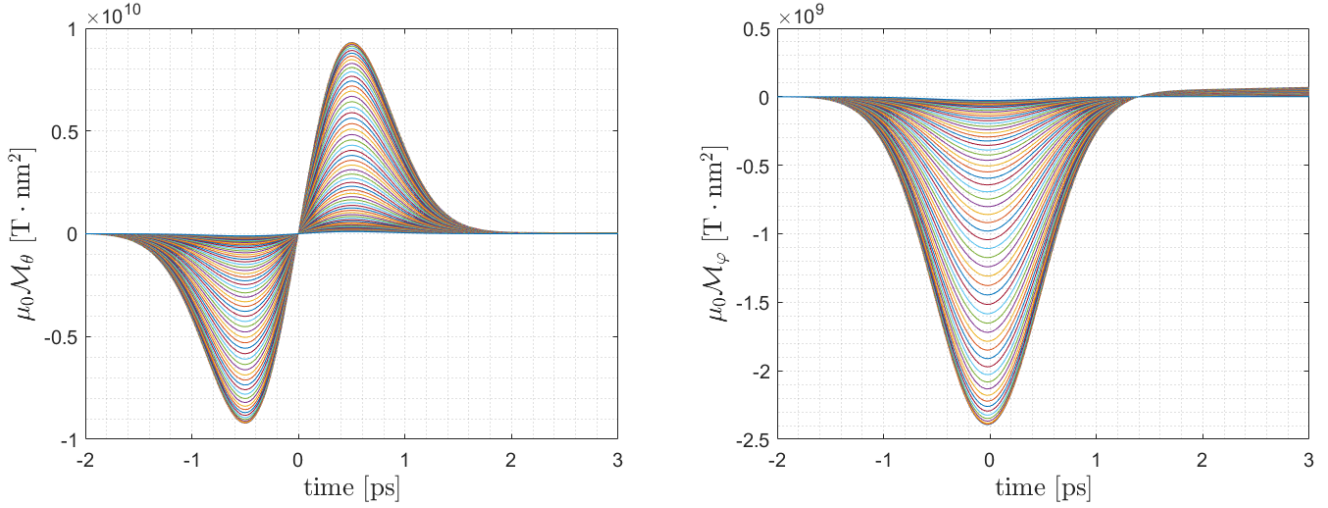


Fig. 5. Amplitude of the spin waves of the system described in the simulation section. Larger curves correspond to spin waves with smaller wave number, the orientation of \mathbf{k} has almost no impact on the dynamic.

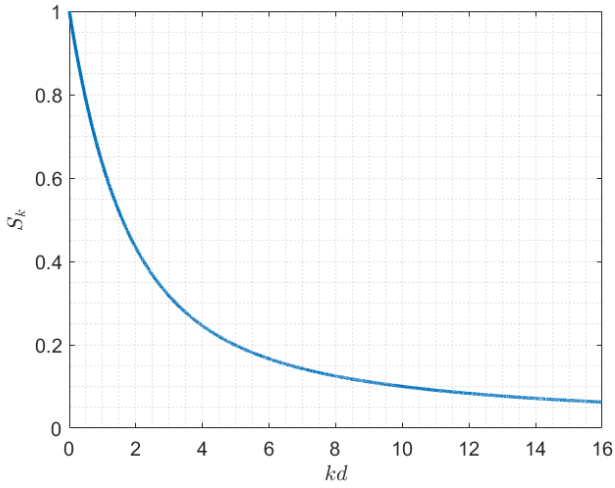


Fig. 6. S_k function defined in (40)

The function S_k is shown in Figure 6. By using the rotated reference frame defined in (12), we obtain the demagnetizing factors used in (17) and (18). They are

$$\begin{aligned}
 D_{\theta\theta} &= (1 - S_k) \cos^2 \theta_M \cos^2 \phi_k + S_k \sin^2 \theta_M , \\
 D_{\theta\varphi} = D_{\varphi\theta} &= \frac{1}{2}(1 - S_k) \cos \theta_M \sin(2\phi_k) , \\
 D_{\varphi\varphi} &= (1 - S_k) \sin^2 \phi_k ,
 \end{aligned} \tag{41}$$

- [2] E. Beaurepaire, J. Merle, A. Daunois, J. Bigot, “Ultrafast Spin Dynamics in Ferromagnetic Nickel”, *Physical Review Letters*, vol. 76, pp. 4250-4253 (1996).

where θ_M is the angle between \mathbf{e}_z and \mathbf{e}_m , and ϕ_k is angle between \mathbf{e}_k and the projection of either \mathbf{e}_θ or \mathbf{e}_m in the xy -plane.

REFERENCES

- [1] J. Walowski and M. Mnzenberg,, “Perspective: Ultrafast magnetism and THz spintronics”, *Journal of Applied Physics*, vol. 120, 140901 (2016).
- [3] A. Kirilyuk, A. V. Kimel, T. Rasing, “Ultrafast optical manipulation of magnetic order”, *Reviews of Modern Physics*, vol. 82, pp. 2731-2784, (2016).
- [4] M. Hudl, M. dAquino, C. Serpico, M. Pancaldi, S.-H. Yang, M.G. Samant, S.S.P. Parkin, H.A. Durr, M.C. Hoffmann, S. Bonetti, “Nonlinear magnetization dynamics driven by strong terahertz fields”, *Physical Review Letters*, vol. 123 , issue 19, pp 197-204 (2019)
- [5] S. Bonetti, M. C. Hoffmann, M. J. Sher, Z. Chen, S. H. Yang, M. G. Samant, S. S. P. Parkin, and H. A. Durr, “THz-Driven Ultrafast Spin-Lattice Scattering in Amorphous Metallic Ferromagnets”, *Physical Review Letters*, vol. 117, 087205, (2016).
- [6] S. J. Gamble, M. H. Burkhardt, A. Kashuba, R. Allenspach, S. S. P. Parkin, H. C. Siegmann, and J. Sth, “Electric Field Induced Magnetic Anisotropy in a Ferromagnet”, *Physical Review Letters*, vol. 102, 217201 (2009).
- [7] H. Suhl, “The theory of ferromagnetic resonance at high signal powers”, *Journal of Physics and Chemistry of Solids*, vol. 1, issue 4, pp. 209-227 (1957)
- [8] G. Bertotti, I.D. Mayergoyz, C. Serpico, “Spin-Wave Instabilities in Large-Scale Nonlinear Magnetization Dynamics”, *Physical Review Letters*, vol. 87, issue 21, pp. 217203 (2001)
- [9] D.D. Stancil, A Prabhakar, “Spin Waves: Theory and Applications”, Springer (2009)